



## Size and shape controlled synthesis of aqueous silver nanoparticles and a comparative study of their fluorescence and electrochemical responses towards cholesterol

Pradyumna Goswami\* and Nilotpal Borah

Department of Chemistry, Gauhati University, Guwahati, Assam, India

---

### ABSTRACT

Five samples of aqueous silver nanoparticles (samples A-E) were synthesized by reducing  $\text{AgNO}_3$  by  $\text{NaBH}_4$  in the presence of poly (vinyl pyrrolidone) (PVP) and sodium citrate. By varying the amount of the stabilizer PVP during synthesis process we get all the five samples of different morphology. We have characterized these samples by TEM, UV-Visible spectroscopy and fluorescence spectroscopy. The fluorescence and electrochemical interactions of these samples towards cholesterol have shown that all the samples behave differently towards cholesterol. By comparing their behaviors towards cholesterol it can be concluded that in future sample A whose fluorescence intensity ( $\lambda_{\text{ex}}=250$  nm;  $\lambda_{\text{emi}}= 220-500$  nm;  $\lambda_{\text{max}} = 341$  nm) enhances 4.3 times of its initial value on interaction with cholesterol can be used as a good fluorescence probe and sample C whose redox potential suffers 148 mV  $-ve$  shift in presence of cholesterol can be used as a good electrochemical probe for the detection of cholesterol in solution.

**Key words:** fluorescence, electrochemical, silver, nanoparticles, cholesterol

---

### INTRODUCTION

Metal nanoparticles display novel physical and chemical properties due to surface effect, where most of the particle atoms are just surface atoms [1]. These novel properties have made metal nanoparticles to play an interesting role in materials technology, biomedicines, catalysis, etc. The optical properties of metal nanoparticles are highly influenced by the preparation methods and conditions, which result in particles of various sizes; shape and surface stabilization [2, 3]. Moreover, some nanoparticles also show interesting electrochemical behaviour. These optical and electrochemical behaviours inspired scientists to develop sensors using metal nanoparticles especially in biomedical field.

Cholesterol is one of such compounds whose sensing has been paid more and more attention in biomedical fields and plays an increasingly important role in improving life quality [4, 5]. Abnormalities of cholesterol levels are symptoms of several diseases, such as hypertension, coronary heart disease, arteriosclerosis, brain thrombosis, lipid metabolism dysfunction and myocardial infarction [6]. Therefore, various research efforts have been given to develop cholesterol sensor [7-12]. Among them, some methods often present certain disadvantages, such as lack of specificity and selectivity. Moreover most of the electrochemical biosensors for cholesterol are enzyme based where enzymes like cholesterol oxidase, cholesterol esterase and peroxidase behaves as intermediate between the analyte cholesterol and the electrode [13-16]. But the enzyme kits are expensive for routine clinical analysis. Therefore, the high cost of enzyme as well as time consumption in analysis restricts the use of this method for routine estimation of cholesterol.

In order to overcome all these problems researchers are trying to use metal nanoparticles to sense cholesterol in a more effective way. The intrinsic properties of metal nanoparticles can be tailored by controlling the size, shape,

composition and crystallinity. Silver nanoparticles are of great interest in a number of disciplines [17-24]. In a reported procedure, aqueous silver nanoparticles were synthesized by reducing  $\text{AgNO}_3$  by  $\text{NaBH}_4$  in the presence of poly (vinyl pyrrolidone) (PVP) and sodium citrate [25]. In this process of synthesis PVP acts as a stabilizer. It is well known that the amount of the stabilizer in the nanoparticles synthesis affects the size and shapes of nanoparticles [26].

As far as we know, there are few reports on the sensing application of silver nanoparticles. Here, we report the synthesis of five samples of silver nanoparticles with different size and shape by varying the amount of PVP in the above mentioned method [25]. We have made a comparative study of the fluorescence and electrochemical sensing of these size and shape controlled silver nanoparticles towards cholesterol. The comparative study indicated that the Ag nanoparticles were promising in fabrication of nonenzymatic cholesterol sensors

## EXPERIMENTAL SECTION

All reagents were purchased from Loba Chemie Pvt Ltd (India). All were of analytical grade and used without any further purification. Double distilled water (prepared by using Rieviera quartz double distillation apparatus) was used for all experiments.

Fluorescence experiments were performed on a Hitachi F-2500 spectrophotometer at room temperature. TEM images were captured using Jeol / JEM-2100 Transmission Electron Microscope.

Voltammetric experiments were carried out at room temperature using CHI 600B Electrochemical Analyzer (USA) in a conventional three electrode system with Ag/AgCl (3M KCl) as the reference electrode, a platinum wire grid as the counter electrode and a glassy carbon (GC) as working electrode. 0.1M  $\text{NaNO}_3$  solution was used as supporting electrolyte. Nitrogen gas was purged through the electrolytic solution for at least 10-15 minutes to remove any dissolved oxygen before every experiment. Nitrogen atmosphere was maintained over the electrolytic solutions during each experiment. The electrode potential values were reported with respect to normal hydrogen electrode, NHE. Prior to every experiment the GC electrode was polished firmly on micro-cloth using fine  $0.05\mu\text{M}$  alumina powders followed by sonication for 2-3 minutes in Millipore water and then rinsed thoroughly with water [27].

### *Synthesis of Silver Nanoparticles*

In our experiment aqueous silver nanoparticles were synthesized by reducing aqueous silver nitrate ( $\text{AgNO}_3$ ) by sodium borohydride ( $\text{NaBH}_4$ ) in the presence of poly(vinyl pyrrolidone) (PVP) and sodium citrate ( $\text{C}_6\text{H}_5\text{Na}_3\text{O}_7$ ) [25]. For this 47.5 mL of double distilled water was deoxygenated by bubbling it with nitrogen gas for 30 min. 0.5 mL of 30 mM aqueous sodium citrate ( $\text{C}_6\text{H}_5\text{Na}_3\text{O}_7$ ) solution was added followed by the addition of 1 mL of 5 mM aqueous  $\text{AgNO}_3$  solution. A 0.5 mL of 5 mM freshly prepared solution of  $\text{NaBH}_4$  was quickly added and the solution immediately turned into a light yellow colour. After nearly 30 s, 'X' mL of aqueous solution of PVP (5%, w/v) was added and the colour of the above solution changed to a darker yellow after the reaction had proceeded for another 30 min. During the entire experiment the solution was stirred vigorously in ice cold conditions. The amount of surfactant plays a crucial role to the formation of nanoparticles with a specific shape and size. Hence, changing the amount of PVP, i.e., X we have prepared 5 samples of silver nanoparticles and these are as follows-

**Table 1: Sampling of silver nanoparticles w.r.t. PVP amount**

Sl. No	Amount of PVP, X in mL	Sample Code
1	0.5	A
2	1.5	B
3	2.5	C
4	3.5	D
5	4.5	E

After synthesis, these PVP capped particles are typically stable for a number of weeks and even months. The morphology of these silver nanoparticles sample (A-E) were viewed under transmission electron microscopy (Fig.1).

TEM images of the sample A (Fig.1A) shows well-separated spherically shaped particles with sizes ranging from 20 nm to 30 nm. The average diameter of the particles is ca. 26 nm. The diffraction pattern of Sample A (images are not shown for all the samples) shows that particles are hexagonal in shape with d-spacing value 0.19 nm.

In sample B it is observed that it contains nano particles of hexagonal, cubic and spherical shapes (Fig.1B). But from the diffraction pattern it is found that particles are mostly cubic in shape with d spacing value 0.22 nm. Moreover, sample B contains lots of massive particles along with the numbers of small particles. The average diameter of the

particles is ranging from 10 to 20 nm; where as in sample C (Fig.1C) almost all the particles are spherical in shape with sizes ranging from 7 nm to 13 nm. No massive particles are observed in this case. The diffraction pattern shows the trigonal planar orientation of these particles with d spacing value 0.21 nm. Sample C also contains some diffused shaped particles (inset).

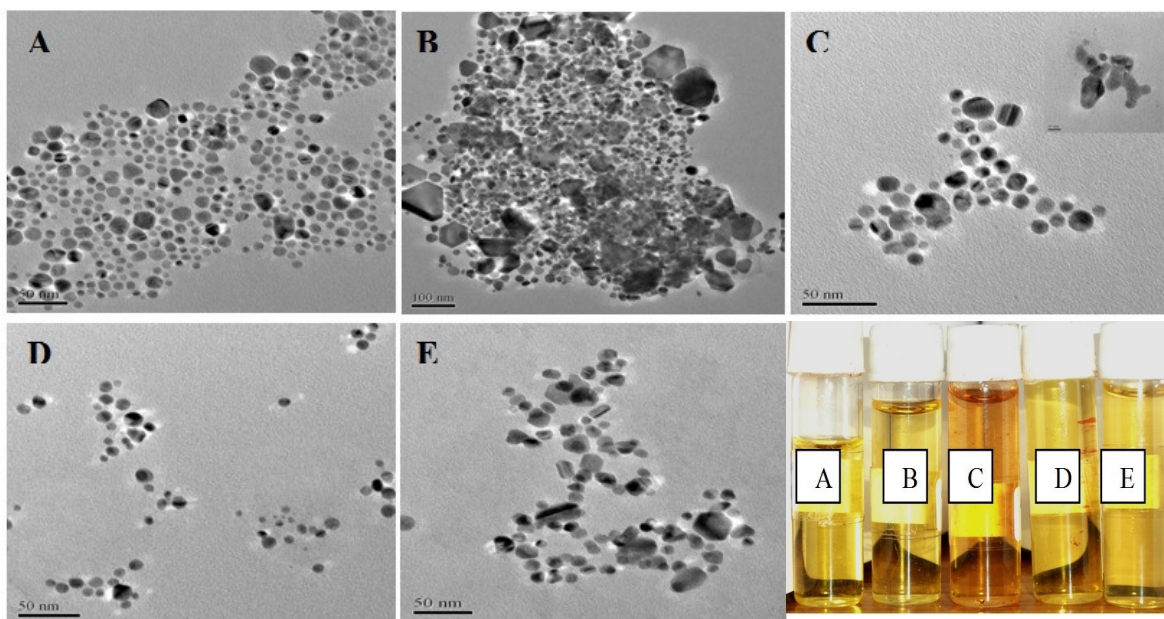


Fig.1: TEM images of silver nanoparticles (sample A-E)

Sample D describes that along with medium sized particle (diameter ranging from 6 nm to 12 nm) it contains lots of very small particles whose diameter ranging from 3 to 6 nm (Fig.1D). The crystallinity of these particles are found to be linear from the diffraction pattern. The d spacing value is 0.24 nm.

But peculiarity is observed in the TEM images of sample E (Fig.1E). It contains particles of different shapes and sizes. Here most of the particles are rod shaped, hexagonal shaped, oval shaped and spherical shaped. It also contains some deformed particles whose shapes can not be predicted. The diffraction pattern shows the linearity in their crystalline structure with d spacing value 0.22 nm. Since the particles are of different shapes, their average sizes can't be determined from the images.

From the TEM images it becomes obvious that all the five samples of silver nanoparticles are of different size and shape. Literature says that these size and shape controlled silver nanoparticles must have different intrinsic properties. We have recorded the absorption spectra of all the five samples of silver nanoparticles in aqueous medium and it has been observed that all the five samples possess individual  $\lambda_{\max}$  which can be considered as characteristic of each sample. Moreover we have recorded the fluorescence emission spectra of five samples of silver nanoparticles in aqueous medium (samples A-E) in the range of 220 - 500 nm by exciting with 250 nm radiation. Although all the samples show fluorescence emission peak at different  $\lambda_{\max}$  vales, except sample A the emission peaks in other samples are not prominent (very low intensities; figures not shown). Sample A shows one fluorescence emission peak with  $\lambda_{\max}$  at 341 nm and with peak intensity 28.93. The difference in the fluorescence spectra may be attributed to the characteristic difference in size, shape and morphology of the five samples of silver nanoparticles.

## RESULTS AND DISCUSSION

### *Interactions of Cholesterol with Fluorescence Spectra of Sample A*

The fluorescence spectrum of sample A was recorded at room temperature using 250 nm photons for excitation (Fig.2). Sample A exhibited an emission band at 220 nm to 500 nm with  $\lambda_{\max}$  at 341 nm (peak intensity 28.93). Addition of 1 mM cholesterol solution into the test sample induced a gradual enhancement in intensity of the fluorescence spectrum of sample A which saturates at 1.0 equivalent (Fig.2). The final enhancement in fluorescence intensity was ca. 4.3 times of the original intensity. Inset of Fig. 2 shows the plot of  $I/I_0$  as a function of cholesterol concentration, where I is the fluorescence intensity at a given concentration of cholesterol and  $I_0$  is the fluorescence intensity at zero concentration of cholesterol in the test solution.

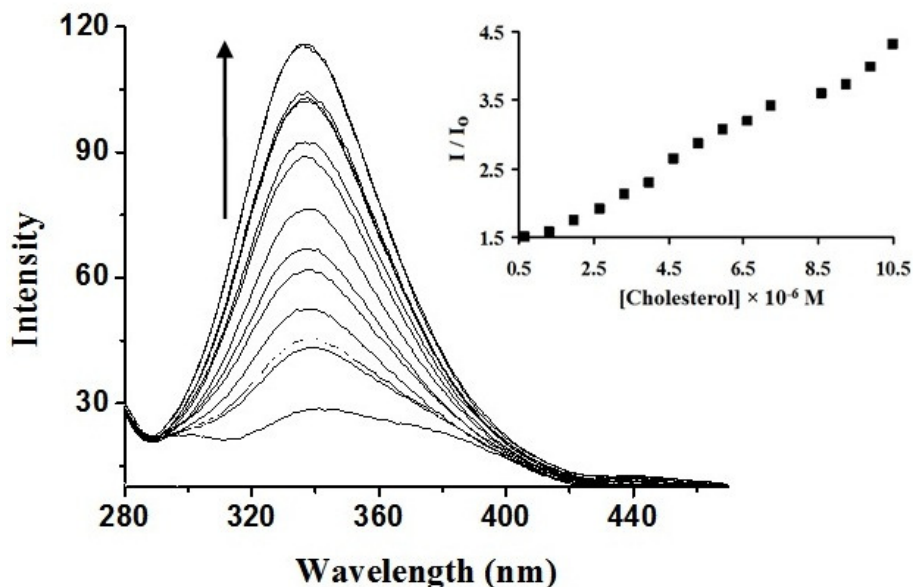


Fig. 2: Fluorescence emission spectra of sample A at different added concentration of cholesterol (saturation value of cholesterol in the test sample is 10.5  $\mu\text{M}$ ) ( $\lambda_{\text{ex}}$ =250 nm;  $\lambda_{\text{em}}$ = 220-500 nm;  $\lambda_{\text{max}}$  = 341 nm; Inset: plot of  $I/I_0$  as a function of cholesterol concentration)

To calculate the binding constant ( $\beta$ ),  $\log\{(I_0-I)/(I-I_{\text{max}})\}$  was plotted versus  $\log[\text{Cholesterol}]$  (Fig.3) [28]; where  $I_0$  is the fluorescence intensity of sample A in absence of cholesterol,  $I$  is the fluorescence intensity of sample A at an added concentration of cholesterol and  $I_{\text{max}}$  is the fluorescence intensity of sample A when concentration of cholesterol attains fluorescence saturation. A least squares fitting of the plot yielded a slope of 1.57 indicates the binding between sample A and cholesterol. The binding constant was calculated to be  $2.9 \times 10^8 \text{ M}^{-1}$ .

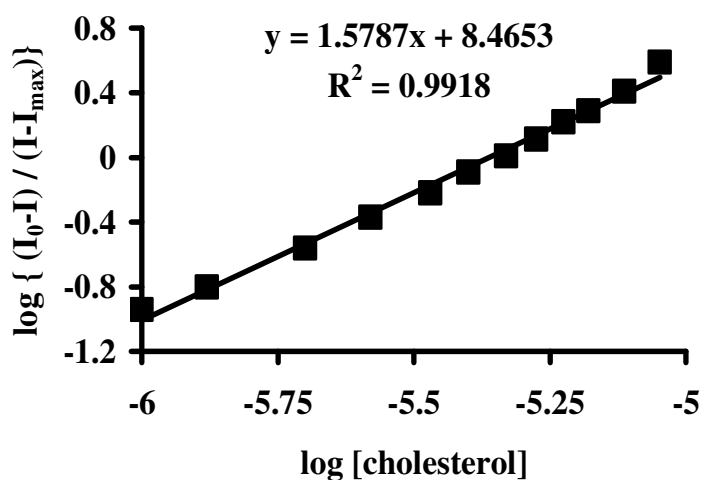
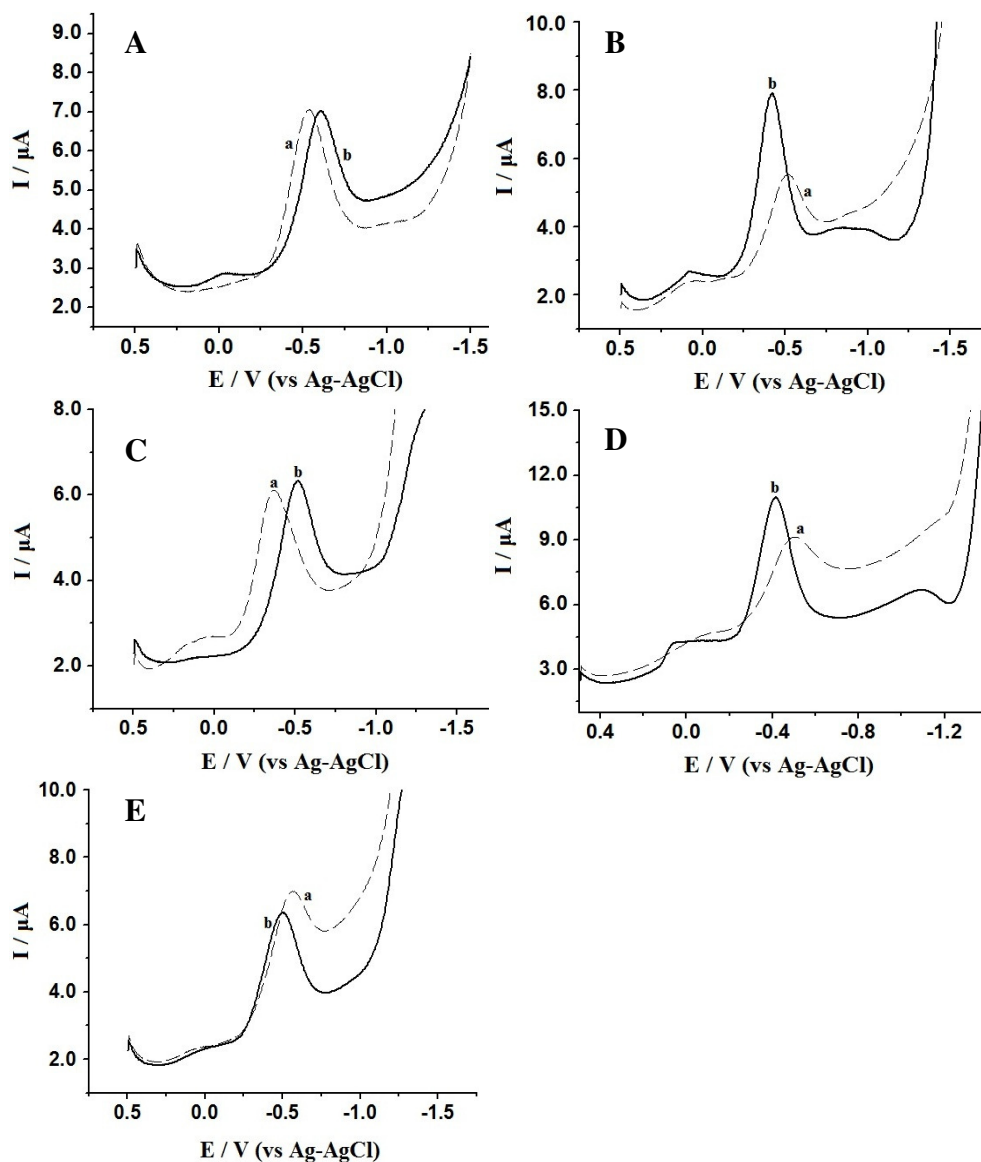


Fig.3: Plot of  $\log\{(I_0-I)/(I-I_{\text{max}})\}$  against  $\log[\text{cholesterol}]$  for sample A

The above mentioned procedures were followed to study the affect of cholesterol on the fluorescence spectra of remaining samples of silver nano particles (sample B-E). But it was found that the fluorescence spectra of other samples were almost unaffected by the presence of cholesterol.

#### **Electrochemical Responses of Silver (Ag) Nanoparticles in Presence of Cholesterol**

Electrochemical responses of all the samples of silver nanoparticles (A-E) were observed using glassy carbon (GC) as the working electrode and Ag-AgCl in 3 M KCl as the reference electrode (Fig.4). It is evident from the figure that the electrochemical behaviours of all the samples of silver nanoparticles (A-E) are different (Fig.4, all curve a). Moreover it is interesting to note that the electrochemical responses of all the samples towards cholesterol are not similar. This peculiarity may be attributed because of the difference in size and shape of the nanoparticles samples.



**Fig.4:** Overlay of square wave voltammograms of (a) pure sample (dashed line) and (b) sample in presence of X M cholesterol (solid line) (WE: GC, Ag-AgCl is the reference electrode). (For A:  $X = 3.32 \times 10^{-6}$  M; for B:  $X = 1.639 \times 10^{-5}$  M; for C:  $X = 1.639 \times 10^{-5}$  M; for D:  $X = 2.755 \times 10^{-5}$  M and for E:  $X = 1.185 \times 10^{-5}$  M)

Fig. 4(A) shows the change in the electrochemical behaviour of sample A on interaction with cholesterol. The curve 'a' in the figure demonstrates the square wave voltammogram (SWV) of pure sample A. It shows a redox peak at potential  $-0.540 \pm 0.005$  V with peak current  $7.048 \times 10^{-6}$  A. On interaction with  $3.32 \times 10^{-6}$  M cholesterol the redox peak shifted to a new potential value  $-0.612 \text{ V} \pm 0.005$  V with peak current  $7.005 \times 10^{-6}$  A. Cholesterol imparts a 72 mV negative shift on the redox potential of sample A. Moreover in SWV of sample A, a new peak was observed at potential  $-0.060 \pm 0.005$  V with peak current  $2.861 \times 10^{-6}$  A in presence of  $3.32 \times 10^{-6}$  M cholesterol.

SWV of sample B was also recorded and shown in 'curve a' of Fig. 4(B). In this case two redox peaks were observed at potentials  $+0.850 \text{ V} \pm 0.005$  V and  $-0.516 \text{ V} \pm 0.005$  V with peak currents  $2.372 \times 10^{-6}$  A and  $5.506 \times 10^{-6}$  A respectively. When we added 1 mM cholesterol solutions to the test sample the redox peak at  $-0.516$  V gradually shifted towards positive and reached a maximum value of  $-0.424 \pm 0.005$  V when cholesterol concentration in the medium was  $1.639 \times 10^{-5}$  M. The peak current of the peak became  $7.860 \times 10^{-6}$  A. The peak at potential  $+0.850$  V remained unaltered in presence of cholesterol in the medium. Unlike sample A where 72 mV negative shift was observed in presence of cholesterol, in this case  $1.639 \times 10^{-5}$  M cholesterol made a 92 mV positive shift on the redox potential of sample B. Besides this, on interaction with cholesterol the redox peak current of sample B also increased by almost 1.4 times.

SWV of sample C in presence of  $1.639 \times 10^{-5}$  M cholesterol was also recorded and this result was compared with pure sample C in Fig. 4(C). Sample C shows two redox peaks at potentials  $+0.095 \text{ V} \pm 0.005 \text{ V}$  and  $-0.368 \text{ V} \pm 0.005 \text{ V}$  with peak currents  $2.552 \times 10^{-6} \text{ A}$  and  $6.028 \times 10^{-6} \text{ A}$  respectively. In presence of  $1.639 \times 10^{-5}$  M cholesterol the redox peak at  $-0.368 \text{ V}$  shifted to a maximum value of  $-0.516 \pm 0.005 \text{ V}$  and the peak current became  $6.315 \times 10^{-6} \text{ A}$ . On interaction with cholesterol sample C loses its redox peak at potential  $+0.095 \text{ V}$ . Here cholesterol imparts a 148 mV negative shift on the redox potential of sample C. This negative shift is greater than twice the negative shift occurs in case of sample A.

The observation of SWV responses of sample D in presence of cholesterol is quite different from the above samples (Fig.4D). In square wave voltammetric experiment, sample D showed one redox peak at potential  $-0.500 \pm 0.005 \text{ V}$  with peak current  $9.064 \times 10^{-6} \text{ A}$  (Fig.4D, curve a). In presence of  $2.755 \times 10^{-5}$  M cholesterol, this redox peak suffered a maximum of 88 mV positive shift and the redox potential became  $-0.412 \pm 0.005 \text{ V}$  with peak current  $10.90 \times 10^{-6} \text{ A}$  (Fig.4D, curve b). Moreover, two additional peaks were observed at potentials  $+0.066 \text{ V} \pm 0.005 \text{ V}$  and  $-1.116 \text{ V} \pm 0.005 \text{ V}$  in presence of  $2.755 \times 10^{-5}$  M cholesterol in the electrolytic medium.

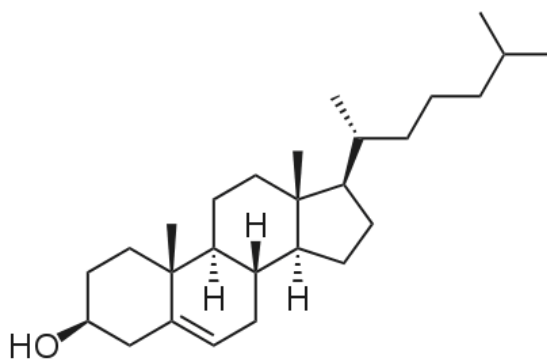
Similarly Fig.4 (E) demonstrates the SWV of pure sample E (curve a) and sample E in presence of  $1.185 \times 10^{-5}$  M cholesterol (curve b). SWV of pure sample E is observed at potential  $-0.570 \text{ V} \pm 0.005 \text{ V}$  with peak current  $6.944 \times 10^{-6} \text{ A}$ . But in this case alike sample D, presence of  $1.185 \times 10^{-5}$  M cholesterol imparts a maximum of 74 mV positive shift in the redox potential of sample E. The new redox potential of sample E in presence of cholesterol became  $-0.496 \text{ V} \pm 0.005 \text{ V}$  with peak current  $6.360 \times 10^{-6} \text{ A}$ . This shift in the redox potential value is the highest which saturates at  $1.185 \times 10^{-5}$  M cholesterol concentration in the electrolytic medium.

A comparison of the electrochemical responses of samples A-E in presence of different added concentration of cholesterol is described in Table 2.

**Table 2. Comparison of SWV responses of five samples of silver nanoparticles (A-E) in presence of different added concentration of cholesterol**

Sl. No	Sample code	E (V) in pure sample	E (V) after addition of cholesterol	Saturated value of cholesterol	Observations
1	A	$E_1 = -0.540$	$E_1 = -0.612$ $E_2 = -0.060$	$3.32 \times 10^{-6} \text{ M}$	72 mV -ve shift
2	B	$E_1 = 0.085$ $E_2 = -0.516$	$E_1 = 0.085$ $E_2 = -0.424$	$1.639 \times 10^{-5} \text{ M}$	92 mV +ve shift
3	C	$E_1 = +0.095$ $E_2 = -0.368$	$E_2 = -0.516$	$1.639 \times 10^{-5} \text{ M}$	148 mV -ve shift
4	D	$E_1 = -0.500$	$E_1 = -0.412$ $E_2 = +0.066$ $E_3 = -1.116$	$2.755 \times 10^{-5} \text{ M}$	88 mV +ve shift
5	E	$E_1 = -0.570$	$E_1 = -0.496$	$1.185 \times 10^{-5} \text{ M}$	74 mV +ve shift

In Table 2 it is seen that the redox behaviour of sample A-E is different in presence of cholesterol in the electrolytic medium. This difference in the redox behaviour of size and shape controlled Ag nanoparticles towards cholesterol reveals an obvious difference in the electrocatalytic behaviour to the oxidation of cholesterol. The most favourable site in cholesterol to be targeted by silver nanoparticles is its lone double bond (Scheme 1) as Ag is prone to form complex containing double bond. The association of Ag with cholesterol will definitely enhance electron density on them (as Ag is  $3d^{10}$  configuration) which might be responsible for the electrocatalytic behaviour of silver towards oxidation of cholesterol.



**Scheme 1: Structure of cholesterol**

Moreover again in Table 2 we have observed that out of these five samples of silver nanoparticles the change in the redox potential of sample C on addition of cholesterol is quite large (148 mV). This significant change of the redox potential can be utilised for a better electrochemical sensing probe for cholesterol in near future.

#### **Interference studies**

Cholesterol is an important component in biological samples. Ascorbic acid, uric acid and glucose are some species that generally interfered with cholesterol determination [29, 30]. We too studied the effect of these three compounds on the fluorescence responses of sample A and electrochemical responses of samples A-E. It was found that up to 1 mM concentration of these compounds in the electrolytic medium the fluorescence emission peak of sample A was not affected (less than 7.8%). Moreover, same concentration of these interfering compounds did not affect the electrochemistry of the sample A-E.

### **CONCLUSION**

In this work we have done a shape and size controlled synthesis of aqueous silver nanoparticles by reducing AgNO<sub>3</sub> by NaBH<sub>4</sub> in the presence of poly (vinyl pyrrolidone) (PVP) and sodium citrate [25]. By varying the amount of PVP (the stabilizer) during the synthesis process we have prepared 5 samples of silver nanoparticles (samples A-E) which differ in their size and shape. The morphological difference can be best viewed by TEM images. The morphological differences lead to the difference in their behaviour which can be easily understood from their absorption spectra, fluorescence spectra and electrochemical responses. We have studied the affect of cholesterol on the fluorescence spectra of these five samples of silver nanoparticles and it was found that only sample A showed a good agreement on the fluorescence spectra. Sample A exhibited an emission band at 220 nm to 500 nm with  $\lambda_{\text{max}}$  at 341 nm (peak intensity 28.93) when excited with 250 nm photon. Addition of 1 mM cholesterol solution into the test sample induced a gradual enhancement in the fluorescence intensity of sample A which saturates at 1.0 equivalent. The final enhancement in fluorescence intensity was ca. 4.3 times of the original intensity which can be utilized for the sensing purpose of cholesterol. The remaining cholesterol samples cannot be used for the fluorescence sensing of cholesterol. The binding constant for sample A was calculated to be  $2.9 \times 10^8 \text{ M}^{-1}$ .

The electrochemical responses of all the samples towards cholesterol are quite interesting. Cholesterol imparts a 72 mV and 148 mV –ve shift in the redox potential of A and C respectively whereas B, D and E suffer +ve shifts of 74 mV, 88 mV and 92 mV respectively. Although the entire nanoparticles samples can be utilized to sense cholesterol electrochemically, it is better to use sample C which shows a remarkable change in its electrochemical behavior (148 mV –ve shift) in presence of  $1.639 \times 10^{-5} \text{ M}$  cholesterol.

#### **Acknowledgement**

This work has been supported by Department of Chemistry (In Dr. Diganta Kumar Das's Lab), Gauhati University. DST, New Delhi is thanked for electrochemical analyzer. Besides, authors thank North Eastern Hill University (NEHU), Shillong for recording TEM images of silver nano particles.

### **REFERENCES**

- [1]N Toshima; LM Liz-Marzan. PV Kamat. (Ed.), *Nanoscale Materials*, Kluwer Academi Pub., London, **2003**; 79-96
- [2]AS Edelstein; RC Cammarata. *Nanomaterials: Synthesis, Properties and Applications*, IOP Pub., London, **1996**
- [3]UKreibig; M Vollmer. *Optical Properties of Metal Clusters*, Springer, Berlin, **1995**
- [4]NA Rakow; KS Suslick. *Nature*, **2000**, 406, 710-715
- [5]SK Arya; PR Solanki; SP Singh; K Kaneto; MK Pandey; M Datta; BD Malhotra. *Biosens Bioelectrons*, **2007**, 22, 2516-2522
- [6]S Aravamudhan; NS Ramgir; S Bhansali. *Sens. Actuators B*, **2007**, 127, 29-34
- [7]RN Qureshi; WT Kok; PJ Schoenmakers. *Anal Chim Acta*, **2009**, 654, 85-94
- [8]P Goswami; K Goswami; DK Das. *J Chem Phram Res*, **2014**, 6(1), 603-610
- [9]B Canabate-Diaz; CA Segura; A Fernandez-Gutierrez; VA Belmonte; FA Garrido; VJL Martinez; MJ Duran. *Food Chem*, **2007**, 102, 593-600
- [10] LC Clark; C Lyons. *Annals of the New York Academy of Sciences*, **1962**, 102, 29-42
- [11] SJ Updike; GP Hicks. *Nature*, **1967**, 214, 986-993
- [12] JH Yu; SQ Liu; HX Ju. *Biosens Bioelectrons*, **2003**, 19, 401-406
- [13] CC Allain; LS Poon. *Clinic Chem*, **1974**, 20, 470-479
- [14] BD Ragland. *Clinic Chem*, **2000** 46, 1848-1853
- [15] J Shen; CC Liu. *Sens Actuators B*, **2007**, 120, 417-427
- [16] S Brahim; D Narinesingh; A Guiseppi-Elie. *Anal Chim Acta*, **2001**, 448, 27-34

- 
- [17] AJ Haes; CL Haynes. *MRS Bulletin*, **2005**, 30, 368-379  
[18] TA Taton; CA Mirkin; RL Letsinger. *Science*, **2000**, 289, 1757-1762  
[19] OD Velev; EW Kaler. *Langmuir*, **1999**, 15, 3693-3702  
[20] AD McFarland; RP Van Duyne; *Nano Letter*, **2003**, 3, 7426-7433  
[21] APAlivisatos. *Nature Biotech*, **2005**, 22, 47-56  
[22] CL Haynes; RP Van Duyne. *J Phys Chem B*, **2003**, 107, 7426-7439  
[23] JJ Macklin; JK Trautman; TD Harris; LE Brus. *Science*, **1996**, 272, 255-262  
[24] YC Cao; R Jin; CA Mirkin. *Science*, **2002**, 297, 1536-1544  
[25] Y Sun; B Mayers; Y Xia. *Nano Letters*, **2003**, 3, 675-681  
[26] W Tu. *Chinese J Polym Sc*, **2008**, 26, 23-30  
[27] J Rajbongshi; DK Das; S Mazumdar. *Electrochim.Acta*, **2010**, 55, 4174-4179.  
[28] K Dutta; DK Das. *Indian J Chem*, **2012**, 51A, 816-820  
[29] Z Matharu; SK Arya; SP Singh; V Gupta; BD Malhotra. *Anal Chim Acta*, **2009**, 634, 243-247.  
[30] T Yu-Chen; S Yun Chen; C-An Lee. *Sens.Actuators B*, **2008**, 135, 96-99.